行政院國家科學委員會專題研究計畫成果報告

1. 紫質的合成，光譜與電催化反應

2. 微過氧化酵素的電化學及電催化反應

計畫類別：☑個別型計畫　□整合型計畫

計畫編號：NSC 88——2113——M002——003

執行期間：87年 8月 1 日至 88 年 7 月 31 日

個別型計畫：計畫主持人：蘇玉龍
共同主持人：

整合型計畫：總計畫主持人：
子計畫主持人：

註：整合型計畫總報告與子計畫成果報告請分開編印各成一冊，彙整一起繳送國科會。

處理方式：☑可立即對外提供參考
（請打∨）□一年後可對外提供參考
□兩年後可對外提供參考
（必要時，本會得展延發表時限）

執行單位：國立台灣大學化學系

中華民國 88 年 12 月 10 日

摘　　要

1. 以電化學方法氧化水溶性之錳紫質，可產生四價及五價之錳紫質。在含氧化態的錳紫質之軸配位水分子具不同之pKa值：$Mn^{IV}(2\text{-}TMPyP)(H_2O)_2$ 為 9.6 與 10.7，$O=Mn^{IV}(2\text{-}TMPyP)(H_2O)$ 則為 10.5。在鹼性溶液中，可以電化學方法產生 $(O)_2Mn^{V}(2\text{-}TMPyP)$，此產物可進行烯類之氧化反應。

2. 在有機溶液中改變軸配位對於錳紫質光譜之影響作電化學研究。首先，陰離子與中心金屬離子之π/σ作用，可經由光譜測定，測出其大小，而氧化度主要在中心金屬上或紫質環，則依軸配位配位基及紫質環上之取代基的拉電子能力而定。對於 $O=Mn^{IV}P$ 的光譜變化可知，氧原子可轉移至烯類化合物。

關鍵詞： 錳紫質，電氧化反應，環氧化反應，烯類氧化

ABSTRACT

1. Electrochemical oxidation of water-soluble manganese(III) *meso*-tetrakis(*N*-methyl-2-pyridyl)porphyrin (Mn^{III}(2-TMPyP)) generates stable Mn^{IV} and Mn^{V} porphyrins. Speciation of various oxidation states of the porphyrin are characterized by spectroelectrochemical methods. The acid dissociation constants (pK_as) for Mn^{III}(2-TMPyP)$(H_2O)_2$ are 9.6 and 10.7, respectively. Spectroelectrochemical results of the one-electron oxidation of Mn^{III}(2-TMPyP) exhibit different forms of oxomanganese(IV) porphyrin, depending on the pH of the solution and the applied potential. The pK_a for O=Mn^{IV}(2-TMPyP)(H_2O) is 10.5. The axial oxygen atom ligated to the Mn(IV) center is protonated in acidic solution (pK_a 3.4). Further one-electron oxidation generates dioxomanganese(V) porphyrin, $(O)_2Mn^{V}$(2-TMPyP), which is stable in alkaline solution at room temperature. No oxidation wave is observed in the cyclic voltammograms, indicating the slow heterogeneous electron transfer rate of these oxidation reactions. The electrogenerated dioxomanganese(V) porphyrin exhibits higher reactivity toward olefin oxidation than oxomanganese(IV) porphyrin in basic solutions. © 1999 Elsevier Science S.A. All rights reserved.

2. A systematic study for the effect of axially coordinated monovalent anions on the electrode reactions of several manganese porphyrins in acetonitrile is presented. Potential shifts of the metal-centered reduction with changes in counterion were related to the degree of Mn(III)-counterion interaction. In the electrochemically induced ligand exchange, perchlorate anion replaces the other anions as axial ligand coordinated to Mn(III) at oxidation potential less than the first oxidation of manganese porphyrins. Formation constants for axial ligation of OH^- are calculated. One-electron oxidation of dihydroxide coordinated manganese porphyrins generate oxomanganese(IV) porphyrin complexes electrochemically. O=Mn^{IV}OEP(OH) is more thermodynamically stable than O=Mn^{IV}TPP(OH), while O=Mn^{IV}TpFPP(OH) cannot be generated electrochemically. In the presence of styrene or cyclohexene, the absorption spectra of oxomanganese(IV) porphyrins are changed to form manganese(III) porphyrins gradually, which indicates the oxygen atom transfer from oxomanganese(IV) porphyrins to the substrates.

Key words: Manganese porphyrin; Electrochemical oxidation; Electrocatalysis; Olefin oxidation

ELSEVIER

www.elsevier.nl/locate/jelechem

Journal of Electroanalytical Chemistry 474 (1999) 52–59

JOURNAL OF ELECTROANALYTICAL CHEMISTRY

Electrochemical characterization and electrocatalysis of high valent manganese *meso*-tetrakis(*N*-methyl-2-pyridyl)porphyrin

Fang-chung Chen [a], Shu-Hua Cheng [b], Chih-Hsing Yu [a], Mao-Huang Liu [a], Y. Oliver Su [a,b,*]

[a] *Department of Chemistry, National Taiwan University, Taipei 106, Taiwan, ROC*
[b] *Department of Applied Chemistry, National Chi Nan University, Nantou Hsien 545, Taiwan, ROC*

Received 11 March 1999; received in revised form 14 June 1999; accepted 2 July 1999

Abstract

Electrochemical oxidation of water-soluble manganese(III) *meso*-tetrakis(*N*-methyl-2-pyridyl)porphyrin (Mn^{III}(2-TMPyP)) generates stable Mn^{IV} and Mn^{V} porphyrins. Speciation of various oxidation states of the porphyrin are characterized by spectroelectrochemical methods. The acid dissociation constants (pK_as) for Mn^{III}(2-TMPyP)$(H_2O)_2$ are 9.6 and 10.7, respectively. Spectroelectrochemical results of the one-electron oxidation of Mn^{III}(2-TMPyP) exhibit different forms of oxomanganese(IV) porphyrin, depending on the pH of the solution and the applied potential. The pK_a for $O{=}Mn^{IV}$(2-TMPyP)(H_2O) is 10.5. The axial oxygen atom ligated to the Mn(IV) center is protonated in acidic solution (pK_a 3.4). Further one-electron oxidation generates dioxomanganese(V) porphyrin, $(O)_2Mn^{V}$(2-TMPyP), which is stable in alkaline solution at room temperature. No oxidation wave is observed in the cyclic voltammograms, indicating the slow heterogeneous electron transfer rate of these oxidation reactions. The electrogenerated dioxomanganese(V) porphyrin exhibits higher reactivity toward olefin oxidation than oxomanganese(IV) porphyrin in basic solutions. © 1999 Elsevier Science S.A. All rights reserved.

Keywords: Manganese porphyrin; Electrochemical oxidation; Electrocatalysis; Olefin oxidation

1. Introduction

Manganese porphyrins have long been studied as model compounds for oxygen transfer reactions of cytochrome P-450 [1–4]. The central metal ion in synthetic manganese porphyrins can exhibit various oxidation states, which are of interest with respect to the chemical reactivity and catalytic properties of the compounds [5,6].

Many high valent metalloporphyrins [7–10] are known to oxidize organic substrates. Manganese porphyrins have shown their high reactivity toward the epoxidation of olefins [11,12] and the hydroxylation of alkanes [13,14]. Most of the systems use chemical oxidants such as molecular oxygen [15,16], iodosylbenzene [17,18], hydrogen peroxide [19,20], alkyl hydroperoxides [21,22], peroxy acids [23] and oxone [24–26]. Only a few studies have developed the oxidation processes electrochemically [3,27]. High oxidation states of oxomanganese(IV) porphyrins and oxomanganese(V) porphyrins are suggested to be involved in the catalytic oxidation reactions [11,28–30].

Groves et al. [11,29] have characterized the high valent oxomanganese(IV) porphyrins by EPR and FT-IR. Spiro et al. [31] identified the vibration frequency of $\nu(Mn^{IV}{=}O)$ by resonance Raman spectra. Recently, oxomanganese(V) porphyrin, $O{=}Mn^{V}$TMPyP(H_2O), was produced from Mn^{III}TMPyP (where TMPyP = *meso*-tetrakis(*N*-methyl-4-pyridyl)porphyrinato dianion) with a variety of oxidants and characterized by stopped-flow spectrophotometry [32]. The oxidation of Mn^{III}(2-TMPyP) (where 2-TMPyP = *meso*-tetrakis(*N*-methyl-2-pyridyl)porphyrinato dianion) with oxone has been previously reported erroneously to afford oxomanganese(IV) porphyrin [25]. The characterization of the oxidation product as oxomanganese(V) porphyrin has been proved by proton NMR [26]. The species, however, is not stable and rapidly converts to oxomangane-

* Corresponding author. Tel.: +886-2-23629809; fax: +886-2-23636359.
E-mail address: yosu@ms.cc.ntu.edu.tw (Y.O. Su)

0022-0728/99/$ - see front matter
PII: S0022-0728(99)00303-4

se(IV) porphyrin, which is relatively stable. The intermediate is then reduced slowly to manganese(III) porphyrin [32]. Oxomanganese(V) porphyrin is more highly reactive toward olefins than oxomanganese(IV) porphyrin, and affords epoxide products [32].

We report here the characterization of manganese *meso*-tetrakis(*N*-methyl-2-pyridyl)porphyrin (Mn(2-TMPyP)) in aqueous buffer solution using electrochemical and spectral methods. The proximity of the positive charges to the porphine causes a strong electron effect on the metalloporphyrins [33–39]. The special properties of this porphyrin makes the detailed speciation of the various oxidation states of oxomanganese porphyrins possible.

2. Experimental

Manganese(III) *meso*-tetrakis(*N*-methyl-2-pyridyl)-porphyrin (Mn^{III}(2-TMPyP)) was synthesized according to literature methods [33–35]. All chemicals were of analytical grade. Buffer solution preparations have been reported elsewhere [36].

Electrochemistry was performed with a Bioanalytical System (West Lafayette, IN) Model CV-27 potentiostat and a BAS X–Y recorder. Cyclic voltammetry was conducted with the use of a three-electrode cell in which a BAS glassy carbon electrode (area = 0.07 cm^2) was used as the working electrode. The auxiliary compartment contained a platinum wire separated by a medium-size glass frit. All cell potentials were taken with the use of a Ag | AgCl | KCl(sat.) reference electrode. The optically-transparent thin-layer electrode (OTTLE) cell was composed of a 1 mm cuvette, a reticular vitreous carbon as the working electrode, a platinum wire as the auxiliary electrode, and a Ag | AgCl | KCl(sat.) reference electrode. UV-vis spectra were measured with a Hewlett-Packard Model 8452A diode array spectrophotometer.

Product analysis was performed with a Waters HPLC system, which was composed of a model 600E multisolvent delivery system, 610E isocratic system, 486 tunable absorbance detector and 746 data module. The substrate, cyclopent-2-ene-1-acetic acid, and the product, cyclopent-2-ene-4-one-1-acetic acid, were separated on a Waters IC-Pac anion HC column. The eluent is a mixture of 1×10^{-3} M Na_2CO_3 and 6×10^{-3} M NaH_2PO_4 at 2.0 ml/min elution rate with detection wavelength at 220 nm.

3. Results and discussion

3.1. pK_a of Mn^{III}(2-TMPyP)$(H_2O)_2$

Fig. 1 shows the spectrophotometric pH titration of Mn^{III}(2-TMPyP) in the range of pH 7.0 to 11.4. The Soret band at 454 nm decreases gradually while a new peak grows at 442 nm. No clear isosbestic point was observed during the titration, suggesting the involvement of two acid/base titration stages. Nonetheless, two sets of absorbance changes with isosbestic points in the 520–620 nm Q band region can be resolved. From the absorbance change at 559 and 548 nm, the two acid dissociation constants of the axial ligated H_2O molecule can be estimated, respectively.

$$Mn^{III}(2\text{-TMPyP})(H_2O)_2 \rightleftharpoons Mn^{III}(2\text{-TMPyP})(H_2O)(OH) + H^+ \qquad pK_{a1} = 9.6$$

$$Mn^{III}(2\text{-TMPyP})(H_2O)(OH) \rightleftharpoons Mn^{III}(2\text{-TMPyP})(OH)_2 + H^+ \qquad pK_{a2} = 10.7$$

It is known that the pK_{a1} and pK_{a2} for Mn^{III}(4-TMPyP) are 10.9 and 12.3 [37], respectively. The lower pK_a for Mn^{III}(2-TMPyP) is attributed to the proximity, and hence stronger electron-withdrawing effect of the pyridinium positive charges to the porphyrin ring.

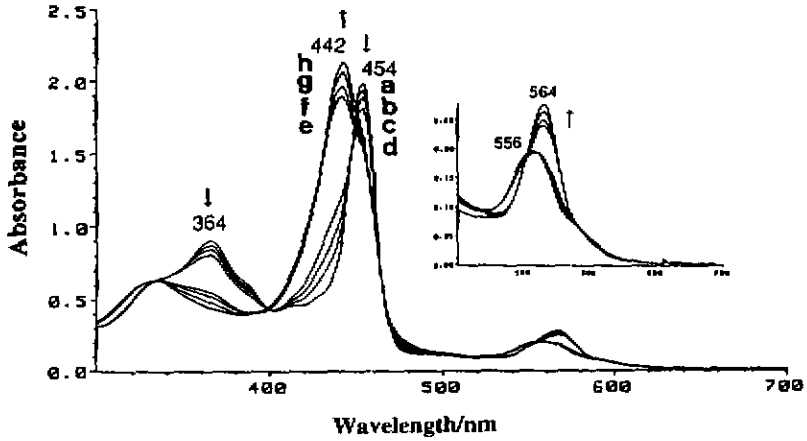

Fig. 1. Spectrophotometric titration of Mn^{III}(2-TMPyP). pH (a) 7.01; (b) 9.25; (c) 9.51; (d) 9.74; (e) 10.63; (f) 10.75; (g) 10.99; (h) 11.44.

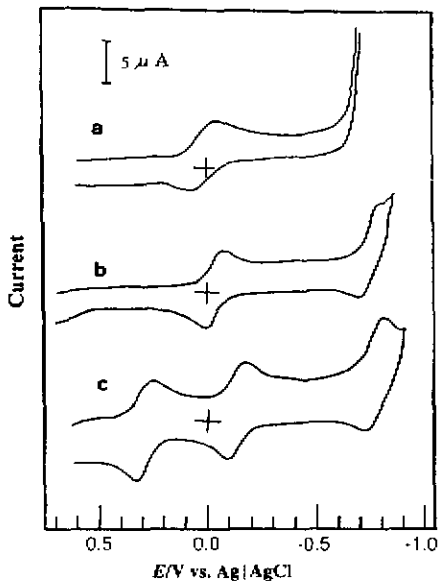

Fig. 2. Cyclic voltammograms of 0.5×10^{-3} M Mn^{III}(2-TMPyP) in pH (a) 3.1; (b) 7.9; (c) 11.6 buffer solutions. Scan rate = 0.1 V s^{-1}.

3.2. Electrochemistry of Mn^{III}(2-TMPyP)

Fig. 2 shows the cyclic voltammograms of Mn^{III}(2-TMPyP) in pH 3.1, 7.9 and 11.6 buffer solutions. A redox couple appears at −0.03 V and an irreversible reduction wave starts at −0.65 V in pH 3.1 solution. The redox potential at −0.03 V is pH dependent and shifts to −0.14 V in pH 11.6 solution. It is thus inferred to be that of the $Mn^{III/II}$(2-TMPyP) redox couple [35].

$$Mn^{III}(2\text{-}TMPyP)(H_2O)(OH) + e^- + H^+ \rightleftharpoons Mn^{II}(2\text{-}TMPyP)(H_2O)_2$$

There is no observable oxidation wave below pH 9. In pH 9.2 solution, a new redox couple appears at +0.53 V, which shifts to +0.28 V as the pH of the solution increases to 11.6. The reactions are thus inferred as the metal-centered oxidation [37].

Fig. 3(a) shows the thin-layer absorption spectral changes during the oxidation of Mn^{II}(2-TMPyP) in pH 9.1 buffer solution. The Soret band at 454 nm decreases gradually and a new broad peak grows at 424 nm with

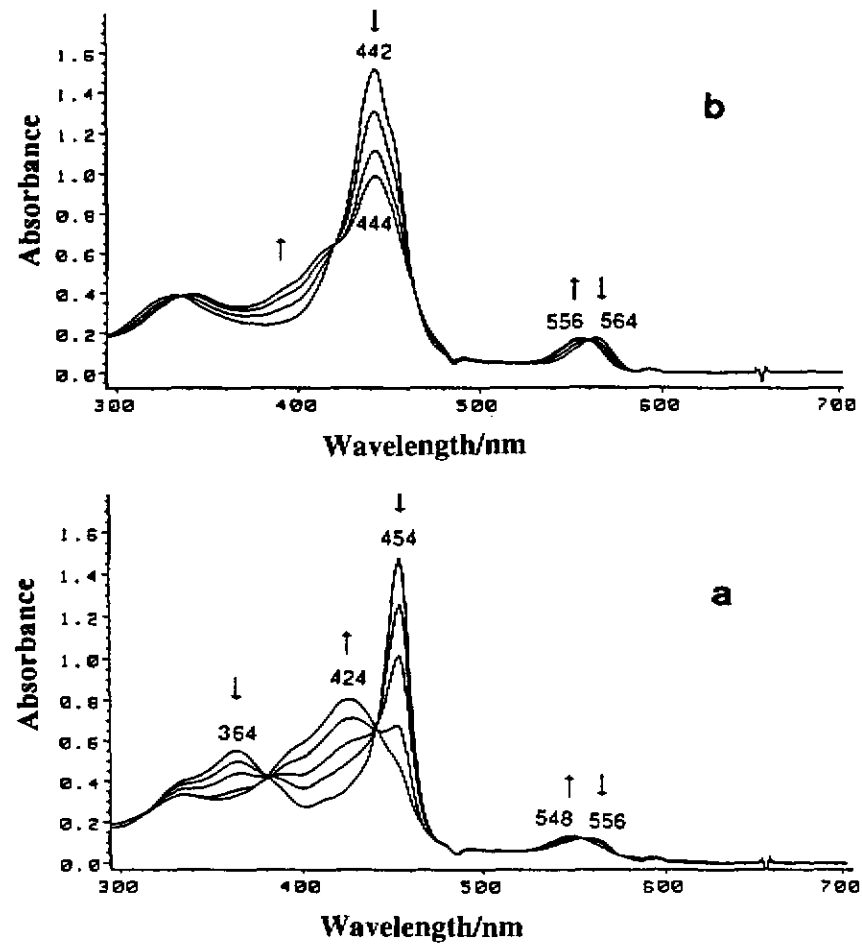

Fig. 3. Time-resolved thin-layer absorption spectral change during the oxidation of Mn^{III}(2-TMPyP) in (a) pH 9.1; (b) pH 12.5 buffer solutions. E_{appl} = (a) +0.85 and (b) +0.50 V.

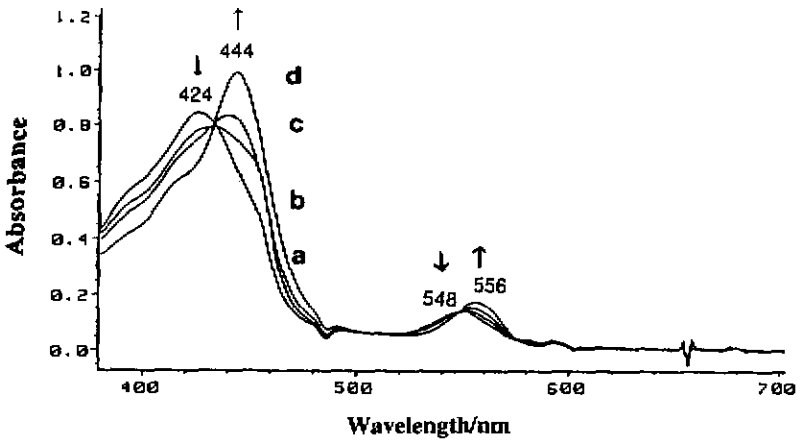

Fig. 4. Spectrophotometric titration of O=Mn^{IV}(2-TMPyP). pH (a) 9.10; (b) 9.92; (c) 10.50 and (d) 12.07.

clear isosbestic points. The species is stable and can be totally reversed to its tri-valent form. In pH 12.5 buffer solution, the oxidation spectrum is quite different (Fig. 3(b)). The Soret band of the final spectrum is at 444 nm and the Q band is at 556 nm. The absorption spectra for the oxidation of Mn^{III}(2-TMPyP) in pH 9.1 and 12.5 buffer solutions are different, indicating a different species of the oxidized form.

Absorption spectral changes in the pH titration of O=Mn^{IV}(2-TMPyP) are shown in Fig. 4. The Soret band shifts from 424 to 444 nm and the Q band shifts from 548 to 556 nm. From the spectrophotometric pH titration, the pK_a is estimated to be 10.5 ± 0.2, which is very close to that obtained from cyclic voltammograms. The equilibrium is thus described as:

$$O{=}Mn^{IV}(2\text{-TMPyP})(H_2O) \rightleftharpoons O{=}Mn^{IV}(2\text{-TMPyP})(OH) + H^+$$

The plot of the redox potential for Mn$^{IV/III}$(2-TMPyP) as a function of pH is shown in Fig. 5. The redox potentials in basic solutions are calculated as the mean of the cathodic and anodic peak potentials of cyclic voltammograms, while in acidic solutions, redox potentials are obtained from spectroelectrochemistry (vide infra: Section 3.3). It appears that slopes are − 115 mV/pH in the range of pH 4.0 to 10.7 and − 60 mV/pH in the range of pH 10.7 to 13.0, respectively. It is thus inferred that two and one proton dissociation occurs upon Mn^{III}(2-TMPyP) oxidation in the respective ranges. Because the pK_a values of Mn^{III}(2-TMPyP)$(H_2O)_2$ are 9.6 and 10.7, respectively, the oxidation reactions are summarized as follows:

$4.0 < pH < 9.6$

$$Mn^{III}(2\text{-TMPyP})(H_2O)_2 \rightleftharpoons O{=}Mn^{IV}(2\text{-TMPyP})(H_2O)_2 + 2H^+ + e^-$$

$9.6 < pH < 10.7$

$$Mn^{III}(2\text{-TMPyP})(H_2O)(OH) \rightleftharpoons O{=}Mn^{IV}(2\text{-TMPyP})(OH) + 2H^+ + e^-$$

$10.7 < pH < 13$

$$Mn^{III}(2\text{-TMPyP})(OH)_2 \rightleftharpoons O{=}Mn^{IV}(2\text{-TMPyP})(OH)_2 + H^+ + e^-$$

The oxidation products are oxomanganese(IV) porphyrins with a H_2O molecule or hydroxide anion coordinated at the sixth position.

3.3. Electro-oxidation of Mn^{III}(2-TMPyP) in acidic solution

Thin-layer absorption spectral changes for the oxidation of Mn^{III}(2-TMPyP) in pH 4.0 buffer solution are

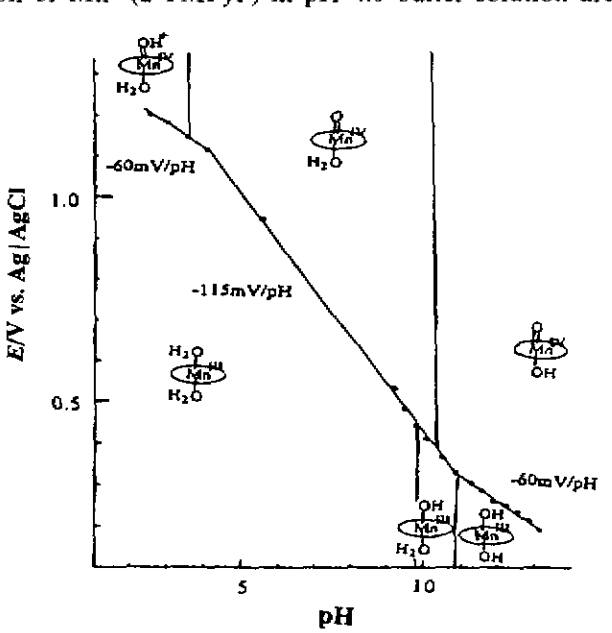

Fig. 5. The redox potential of Mn$^{IV/III}$(2-TMPyP) as a function of pH.

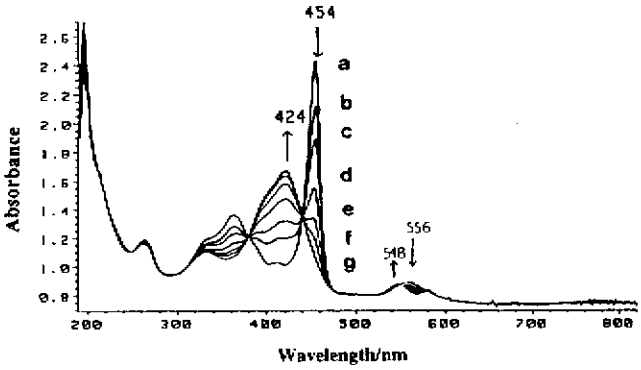

Fig. 6. Thin-layer absorption spectral changes of 1.0×10^{-4} M Mn^{III}(2-TMPyP) at different oxidation potentials in pH 4.0 buffer solution. E_{appl} = (a) 0.40; (b) 1.08; (c) 1.10; (d) 1.12; (e) 1.14; (f) 1.16 and (g) 1.25 V.

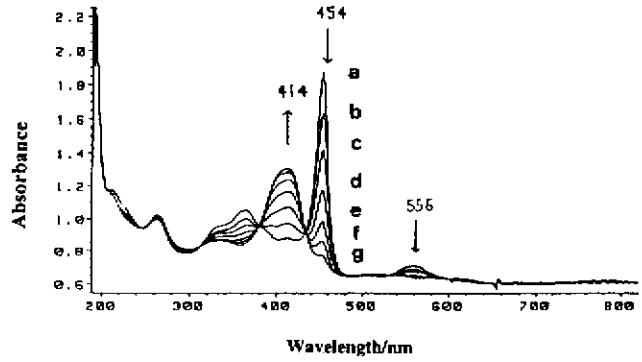

Fig. 7. Thin-layer absorption spectral changes of 1.0×10^{-4} M Mn^{III}(2-TMPyP) at different oxidation potentials in pH 2.5 buffer solution. E_{appl} = (a) 0.40; (b) 1.18; (c) 1.20; (d) 1.22; (e) 1.24; (f) 1.26 and (g) 1.30 V.

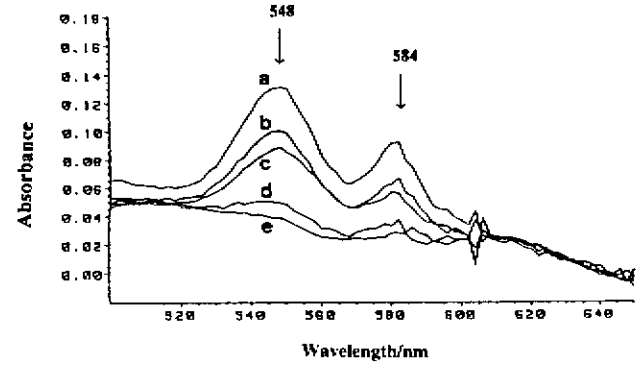

Fig. 8. Q band absorption spectral changes of Mn^{IV}(2-TMPyP) in solutions of various pH values. pH (a) 4.00; (b) 3.75; (c) 3.50; (d) 2.70; (e) 2.50.

shown in Fig. 6. The final spectrum at +1.25 V is identical with that obtained in Fig. 3(a) (pH 9.1). The reaction involves a one-electron oxidation [38,39]. Thus, the oxidation species is formulated as O=Mn^{IV}(2-TMPyP)(H_2O), and the formal potential is calculated as +1.12 V, which is very close to the reported formal potential of one-electron oxidation of manganese(III) *meso*-tetrakis(2,6-dichloro-3-sulfonatophenyl)-porphyrin [40]. The oxomanganese(IV) porphyrin will return to Mn^{III}(2-TMPyP)(H_2O)$_2$ rapidly and reversibly under open circuit without any decrease in absorbance. A similar absorption spectrum is also achieved for the oxidation of Mn^{III}(2-TMPyP) in pH 5.5 buffer solution. The formal potential is calculated as +0.95 V [41].

Cyclic voltammograms of Mn^{III}(2-TMPyP) in pH < 9 solutions do not show any oxidation waves in the potential range of +0.2 to +1.3 V even at scan rates lower than 10 mV s^{-1}. Nonetheless, OTTLE experiments on the oxidation of Mn^{III}(2-TMPyP) in acidic solution have made the calculation of the formal potential possible [41]. The results indicate a slow heterogeneous electron-transfer rate for Mn^{III}(2-TMPyP)(H_2O)$_2$ oxidation.

Thin-layer absorption spectral changes of oxidation of Mn^{III}(2-TMPyP) in pH 2.5 buffer solution are shown in Fig. 7. The Soret band decreases at 454 nm while a new broad peak grows at 414 nm. The Q band at 556 nm becomes featureless upon oxidation. The oxidized species is stable at +1.30 V, and returns reversibly to Mn^{III}(2-TMPyP)(H_2O)$_2$. The final spectrum of the oxidized species is quite different from those of O=Mn^{IV}(2-TMPyP)(H_2O) and O=Mn^{IV}(2-TMPyP)(OH). The formal potential for the oxidation of Mn^{III}(2-TMPyP) in pH 2.5 buffer solution is calculated as +1.20 V. The slope of the redox potentials for $Mn^{IV/III}$(2-TMPyP) vs. pH is about 60 mV/pH in the range of pH < 4 (Fig. 5), indicating a one-proton dissociation upon Mn^{III}(2-TMPyP)(H_2O)$_2$ oxidation. Thus, the oxidized form is inferred to be H^+O=Mn^{IV}(2-TMPyP)(H_2O) and the oxidation reaction is shown below:

$$Mn^{III}(2\text{-TMPyP})(H_2O)_2 \rightleftharpoons H^+O=Mn^{IV}(2\text{-TMPyP})(H_2O) + H^+ + e^-$$

Fig. 8 shows the Q-band spectral changes for Mn^{III}(2-TMPyP) oxidation under various acidic conditions. The absorbance of the Q band decreases as the pH of the solution decreases. Based on the absorbance at 548 nm, the pK_a of the protonated oxomanganese(IV) porphyrin is calculated.

$$H^+O=Mn^{IV}(2\text{-TMPyP})(H_2O) \rightleftharpoons O=Mn^{IV}(2\text{-TMPyP})(H_2O) + H^+ \qquad pK_a = 3.4$$

Various forms of Mn^{III}(2-TMPyP) and the oxomanganese(IV) porphyrin are thus shown in the $E^{\circ\prime}$ versus pH diagram for $Mn^{IV/III}$(2-TMPyP) (Fig. 5). Scheme 1 presents all the reactions in this study and the absorption wavelengths of the various species are listed in Table 1.

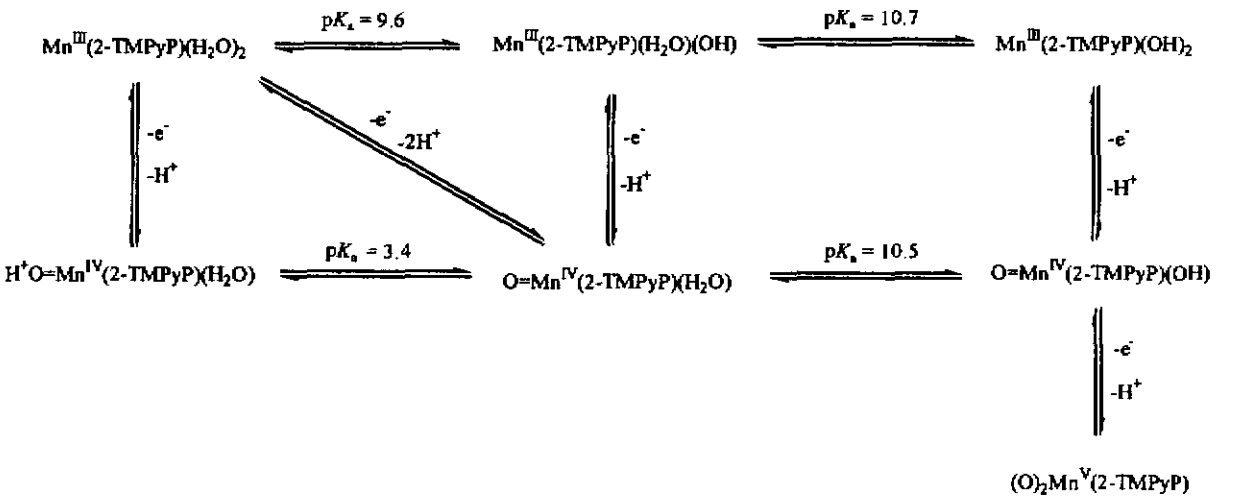

Scheme 1.

Table 1
Absorption spectra of various oxidation states of Mn(2-TMPyP) species

Species	B band λ/nm ($10^{-3}\varepsilon$/l mol^{-1} cm^{-1})	Q band λ/nm ($10^{-3}\varepsilon$/l mol^{-1} cm^{-1})
$Mn^{III}(2\text{-}TMPyP)(H_2O)_2$	454 (91.7)	556 (11.6)
$Mn^{III}(2\text{-}TMPyP)(OH)_2$	442 (99.8)	564(15.4)
$O{=}Mn^{IV}(2\text{-}TMPyP)(H_2O)$	424 (55.1)	548 (9.4)
$O{=}Mn^{IV}(2\text{-}TMPyP)(OH)$	444 (64.7)	556 (11.5)
$H^+O{=}Mn^{IV}(2\text{-}TMPyP)(H_2O)$	414 (49.5)	–
$(O)_2Mn^{V}(2\text{-}TMPyP)$	432 (113.4)	548 (15.0)

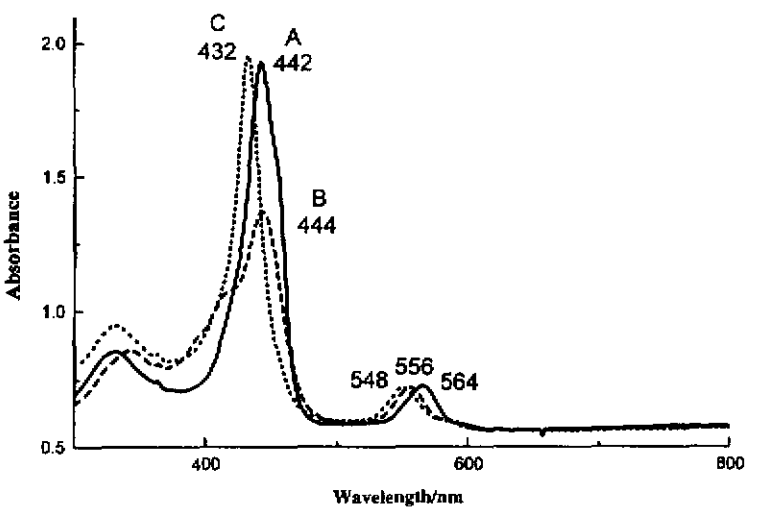

Fig. 9. Absorption spectra of $Mn^{III}(2\text{-}TMPyP)$, $Mn^{IV}(2\text{-}TMPyP)$ and $Mn^{V}(2\text{-}TMPyP)$ in pH 12.0 buffer solution obtained at E_{appl} = (A) +0.10 (—); (B) +0.40 (---) and (C) +0.92 (···) V.

3.4. Electrochemical generation of $Mn^{V}(2\text{-}TMPyP)$

The electro-oxidation of $Mn^{III}(2\text{-}TMPyP)$ in pH 12 buffer solution is monitored by OTTLE (Fig. 9). At +0.40 V, the absorption spectrum with a broad Soret band indicates the formation of $O{=}Mn^{IV}(2\text{-}TMPyP)(OH)$ [37]. At +0.92 V, a new band of higher absorbance appears at 432 nm. The peak is sharper than that of $O{=}Mn^{IV}(2\text{-}TMPyP)(H_2O)$ and $O{=}Mn^{IV}(2\text{-}TMPyP)(OH)$ and the peak wavelength is different. The

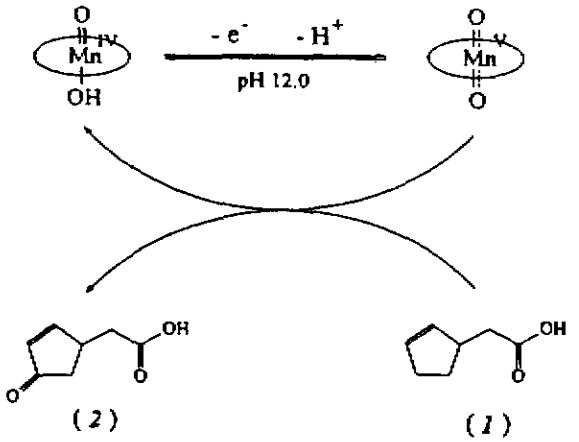

Scheme 2.

oxidation potential for Mn^{IV}(2-TMPyP) decreases as the pH of the solution increases, suggesting a proton transfer upon oxidation. Thus, the oxidation reaction is metal-centered and shown below:

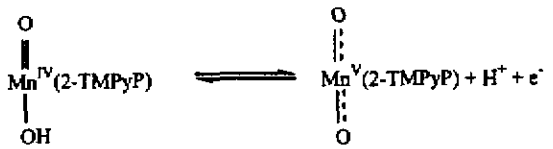

Groves et al. [26,32] have used chemical oxidants to achieve high valent oxomanganese(V) porphyrin, formulated as $O=Mn^{V}TMPyP(H_2O)$, in pH 7.4 phosphate buffer. In our studies, more basic solutions were used (pH 12–14). Deprotonation of the axial H_2O molecule or hydroxide anion will generate the dioxo species. To our knowledge, this is the first stable dioxomanganese(V) porphyrin, which is generated electrochemically in aqueous solution at room temperature. In neutral solutions, similar dioxomanganese(V) porphyrin is also achieved but with smaller absorbance in the Soret band, suggesting decomposition during the oxidation reaction. Chemical oxidation of Mn^{III}(2-TMPyP) in 1 M NaOH by $KHSO_5$ gives an absorption spectrum identical to the final spectrum in Fig. 9. After a few minutes, the species changes to $O=Mn^{IV}$(2-TMPyP)-(OH).

An attempt to characterize the axial vibration of Mn^{V}(2-TMPyP) by resonance Raman spectroscopy, however, did not succeed. Though the spectral pattern of Mn^{V}(2-TMPyP) is a little different from that of Mn^{IV}(2-TMPyP), it appears that no corresponding stretching frequency for the axial ligand vibration of Mn^{V}(2-TMPyP) could be observed. The stretching frequency at 725 cm^{-1} resulted from photoreduction of Mn^{V}(2-TMPyP) to Mn^{IV}(2-TMPyP) [31]. More work will be done to characterize the axial vibration of Mn(V) porphyrins.

3.5. Electrocatalytic oxidation of olefins by Mn^{V}(2-TMPyP)

The reaction of electrogenerated $O=Mn^{IV}$(2-TMPyP)(H_2O) with an olefin substrate, cyclopent-2-ene-1-acetic acid (1), leading to the formation of an oxidation product, cyclopent-2-ene-4-one-1-acetic acid (2), in acidic solutions has been reported [41]. However, the absorption spectrum of Mn^{III}(2-TMPyP) in pH 12 solution in the presence of substrate (1) at +0.40 V is the same as that without substrate (1). The results indicate that the electrogenerated $O=Mn^{IV}$(2-TMPyP)(OH) in strong alkaline solutions does not react with the substrate.

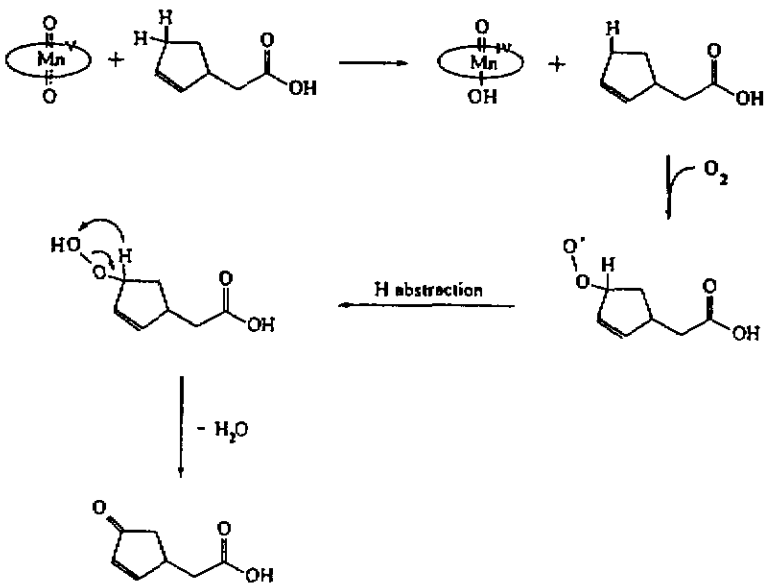

Scheme 3.

Bulk electrolysis of substrate (1) with Mn^{III}(2-TMPyP) was conducted at +1.30 V in pH 2.5 buffer solution for 3 h. Product analysis showed that product (2) is less than that obtained in pH 5.5 buffer solution [41]. The phenomena indicate that protonated oxomanganese(IV) porphyrin, $H^+O=Mn^{III}$(2-TMPyP)(H_2O), is a weaker catalyst than $O=Mn^{IV}$(2-TMPyP)(H_2O).

At higher oxidation potentials, where $(O)_2Mn^V$(2-TMPyP) is generated, the absorption spectrum is quite different for solutions with and without substrate (1). In the absence of substrate (1), the absorption spectrum of Mn^{III}(2-TMPyP)$(OH)_2$ changes to form $(O)_2Mn^V$(2-TMPyP) at +0.92 V in pH 12.0 buffer solution. While in the presence of substrate (1), the final spectrum is similar to that of $O=Mn^{IV}$(2-TMPyP)(OH) at the same applied potential. The results suggest a rapid reaction occurs between $(O)_2Mn^V$(2-TMPyP) and substrate (1) with the porphyrin finally returning to its $O=Mn^{IV}$(2-TMPyP)(OH) state, which does not react with substrate (1).

Bulk electrolysis of substrate (1) in the presence of Mn^{III}(2-TMPyP) at pH 12.0 buffer solution supports the above speculations. After electrolysis at +0.40 V for 2 h, the chromatogram is the same as that before electrolysis. During electrolysis at +0.92 V for 2 h, product (2) is generated with higher yield under air than that obtained under N_2. The higher reactivity of oxomanganese(V) porphyrin than oxomanganese(IV) porphyrin toward alkene epoxidation has been reported by Groves et al. [32]. The proposed mechanism for the catalytic reaction is thus shown in Schemes 2 and 3 [42,43].

Acknowledgements

This work was supported by the National Science Council and the Ministry of Education of the Republic of China. Helpful discussions from Thomas Spiro at Princeton University is gratefully acknowledged.

References

[1] B. Meunier, M.E. De Carvalho, O. Bortolini, M. Momenteau, Inorg. Chem. 27 (1988) 161.
[2] S. Banfi, F. Montanari, S. Quici, J. Org. Chem. 53 (1988) 2863.
[3] H. Nishihara, K. Pressprich, R.W. Murray, J.P. Collman, Inorg. Chem. 29 (1990) 1000.
[4] J.T. Groves, Y.-Z. Han, in: P.R. Oritz de Montellano (Ed.), Cytochrome P-450. Structure, Mechanism and Biochemistry, Plenum Press, New York, 1995.
[5] M. Calvin, Science 184 (1974) 375.
[6] A. Harriman, Coord. Chem. Rev. 28 (1979) 147.
[7] J.E. Penner-Hahn, K.S. Elbe, T.J. McMurry, M.R. Renner, A.L. Balch, J.T. Groves, J.H. Dawson, K.O. Hodgson, J. Am. Chem. Soc. 108 (1986) 7819.
[8] J.E. Penner-Hahn, M. Benfatto, B. Hedman, T. Takahashi, D. Sebastian, J.T. Groves, K.O. Hodgson, Inorg. Chem. 25 (1986) 2255.
[9] A.L. Balch, G.N. La Mar, L. Latos-Grazynski, M.W. Renner, V. Thanabal, J. Am. Chem. Soc. 107 (1985) 3003.
[10] R.A. Sheldon (Ed.), Metalloporphyrins in Catalytic Oxidations, Marcel Dekker, New York, 1994.
[11] J.T. Groves, M.K. Stern, J. Am. Chem. Soc. 110 (1988) 8638.
[12] S. Banfi, M. Cavazzini, F. Coppa, S.V. Barkanova, O.L. Kaliya, J. Chem. Soc. Perkin. Trans. II (1997) 1577.
[13] J.T. Groves, Y. Watanabe, T.J. McMurry, J. Am. Chem. Soc. 105 (1983) 4489.
[14] J.T. Groves, Y. Watanabe, Inorg. Chem. 25 (1986) 4808.
[15] I. Tabushi, M. Kodera, J. Am. Chem. Soc. 108 (1986) 1101.
[16] S.E. Creager, S.A. Raybuck, R.W. Murray, J. Am. Chem. Soc. 108 (1986) 4225.
[17] C.L. Hill, J.A. Smegal, T.J. Henly, J. Org. Chem. 48 (1983) 3277.
[18] J.T. Groves, W.J. Kruper, R.C. Haushaulter, J. Am. Chem. Soc. 102 (1980) 6375.
[19] J.P. Renaud, P. Battioni, J.F. Bartoli, D. Mansuy, J. Chem. Soc. Chem. Commun. (1985) 888.
[20] P. Battioni, J.P. Renaud, J.F. Bartoli, D. Mansuy, J. Chem. Soc. Chem. Commun. (1986) 341.
[21] D. Mansuy, P. Battioni, J.P. Renaud, J. Chem. Soc. Chem. Commun. (1984) 1255.
[22] D. Mansuy, J.F. Bartoli, M. Momenteau, Tetrahedron Lett. 23 (1982) 2781.
[23] K. Ichihara, Y. Naruta, Chem. Lett. 2 (1998) 185.
[24] J. Bernadou, A.S. Fabiano, A. Robert, B. Meunier, J. Am. Chem. Soc. 116 (1994) 9375.
[25] N.W.J. Kamp, J.R. Lindsay Smith, J. Mol. Catal. A Chem. 113 (1996) 131.
[26] J.T. Groves, N. Jin, J. Am. Chem. Soc. 121 (1999) 2923.
[27] C.-Y. Lin, Y.O. Su, J. Electroanal. Chem. 265 (1989) 305.
[28] K.R. Rodgers, H.M. Goff, J. Am. Chem. Soc. 109 (1987) 611.
[29] J.T. Groves, M.K. Stern, J. Am. Chem. Soc. 109 (1987) 3812.
[30] M. Schappacher, R. Weiss, Inorg. Chem. 26 (1987) 1190.
[31] R.S. Czernuszewicz, Y.O. Su, M.K. Stern, D.K. Macro, D. Kim, J.T. Groves, T.G. Spiro, J. Am. Chem. Soc. 110 (1988) 4158.
[32] J.T. Groves, J. Lee, S.S. Marla, J. Am. Chem. Soc. 119 (1997) 6269.
[33] P. Hambright, T. Gore, M. Burton, Inog. Chem. 15 (1976) 2314.
[34] J. Davila, A. Harriman, M.-C. Richoux, L.R. Milgom, J. Chem. Soc. Chem. Commun. (1987) 525.
[35] C.-H. Yu, Y.O. Su, J. Electroanal. Chem. 368 (1994) 323.
[36] S.-M. Chen, Y.O. Su, J. Electroanal. Chem. 280 (1990) 189.
[37] C.-Y. Lin, Z.-F. Lin, T.-M. Hseu, Y.O. Su, J. Chin. Chem. Soc. 37 (1990) 335.
[38] D.F. Rohrbach, E. Deutsch, W.R. Heineman, R.F. Pasternack, Inorg. Chem. 16 (1977) 2650.
[39] S.-M. Chen, Y.O. Su, J. Chem. Soc. Chem. Commun. (1990) 491.
[40] S. Jeon, T.C. Bruice, Inorg. Chem. 31 (1992) 4843.
[41] M.-H. Liu, Y.O. Su, J. Chem. Soc. Chem. Commun. (1994) 971.
[42] Y.-H. Lu, Y.O. Su, J. Electroanal. Chem. 446 (1998) 25.
[43] M.-H. Liu, Y.O. Su, J. Electroanal. Chem. 452 (1998) 113.

Axial Ligand Effects on the Redox Reactions of Manganese Porphyrins

Chi-Hong Chang[a] (張志宏), Shu-Hua Cheng[b]* (鄭淑華) and Y. Oliver Su[a]* (蘇玉龍)
[a]*Department of Chemistry, National Taiwan University, Taipei, Taiwan 106, R.O.C.*
[b]*Department of Cosmetic Science, Chia Nan College of Pharmacy and Science, Tainan, Taiwan 717, R.O.C.*

A systematic study for the effect of axially coordinated monovalent anions on the electrode reactions of several manganese porphyrins in acetonitrile is presented. Potential shifts of the metal-centered reduction with changes in counterion were related to the degree of Mn(III)-counterion interaction. In the electrochemically induced ligand exchange, perchlorate anion replaces the other anions as axial ligand coordinated to Mn(III) at oxidation potential less than the first oxidation of manganese porphyrins. Formation constants for axial ligation of OH^- are calculated. One-electron oxidation of dihydroxide coordinated manganese porphyrins generate oxomanganese(IV) porphyrin complexes electrochemically. $O=Mn^{IV}OEP(OH)$ is more thermodynamically stable than $O=Mn^{IV}TPP(OH)$, while $O=Mn^{IV}TpFPP(OH)$ cannot be generated electrochemically. In the presence of styrene or cyclohexene, the absorption spectra of oxomanganese(IV) porphyrins are changed to form manganese(III) porphyrins gradually, which indicates the oxygen atom transfer from oxomanganese(IV) porphyrins to the substrates.

INTRODUCTION

Manganese porphyrins have long been studied as model compounds for monooxygenase and peroxidases which play key roles in electron transfer processes in several biological systems.[1-6] The metal ion in synthetic manganese porphyrins can exist in various oxidation states. It is of interest with respect to the particular chemical reactivity and catalytic properties of these compounds.[7-9]

In 1982, Kelly and Kadish[10] reported effects of solvent and axially coordinated anions on the electrode reactions of manganese porphyrins. On the basis of their results, complete dissociation of axial ligand of ClO_4^- from $Mn^{III}TPP(ClO_4)$ in strongly coordinating solvent has been reported.

$$Mn^{III}TPP(ClO_4) = Mn^{III}TPP^+ + ClO_4^-$$
$$Mn^{III}TPP(ClO_4) + xS = Mn^{III}TPP(S)_x^+ + ClO_4^-$$
S: solvent

In solvents of dielectric constants lower than 10.7, associated $Mn^{III}TPP(ClO_4)$ rather than $[Mn^{III}TPP]^+$ is the major species in solution. In nonbonding solvents, such as CH_2Cl_2 and $C_2H_4Cl_2$, the reduction of $Mn^{III}TPP(X)$ (where X = ClO_4^-, I^-, SCN^-, Br^-, Cl^- and N_3^-) became more difficult by the increase of Mn^{III}-X binding strength. The reduction potential difference between $Mn^{II/III}TPP(ClO_4)$ and $Mn^{II/III}TPP(N_3)$ is about 180 mV. In medium coordinating solvent, such as CH_3CN, the difference is only 100 mV. In strongly coordinating solvent, such as pyridine, the difference is lowered to 20 mV.

Groves and Stern[8] have isolated and characterized two types of oxomanganese(IV) porphyrin complexes formulated as $Mn^{IV}TMP(O)$ and $Mn^{IV}TMP(O)(OH)$ (where TMP = the dianion of 5,10,15,20-tetramesitylporphyrin). The high valent manganese porphyrins were produced from a mixture of $Mn^{III}TMP(Cl)$ and tetra-*n*-butylammonium hydroxide (TBA(OH)) chemically or electrochemically. TBA(OH) is used as the source of hydroxide anion and hence oxygen atom.

Although oxidation of hydroxide anion coordinated manganese porphyrin have been reported,[8] the coordination between hydroxide anion and manganese porphyrin is not clear. This paper presents the results of such studies. Acetonitrile (CH_3CN) instead of methanol was used as solvent for TMA(OH) titration and all electrochemical experiments to prevent the competition of CH_3OH[11] and OH^- as the fifth and sixth ligand on the Mn(III) central ion. Also, this paper presents the axial ligation ability of hydroxide anion on manganese porphyrins. The ligation abilities for OH^-, ClO_4^-, Cl^- and OAc^- on manganese porphyrins are compared and the formation constants of OH^- on manganese porphyrins are calculated. Four different anions were coordinated to three types of manganese porphyrins, and their redox reactions were investigated in acetonitrile. Mechanisms of oxidation and reduction reactions are presented.

EXPERIMENTAL

Methods

Cyclic voltammetric experiments were conducted with

a EG & G Princeton Applied Research Model 174A polarographic analyzer and EG & G PARC Model 175 Universal Programmer. The three-electrode electrochemical cell contained a Pt working electrode (Bioanalytical System, BAS, IN. USA), a Pt-wire counter electrode, and a homemade saturated Ag/AgCl as a reference electrode. All potentials were recorded vs. Ag/AgCl. A BAS X-Y recorder was used to record the current-voltage output.

For all electrochemical experiments, the reference electrode was separated from the bulk solution by a glass fritt filled with solvent and a supporting electrolyte. Deaeration of all solutions was accomplished by passing a constant stream of high-purity nitrogen through the solution for 10 min and by maintaining a blanket of the gas over the solution during the experiment.

UV-visible spectra were measured with a Hewlett Packard Model 8452A Spectrophotometer. The OTTLE (optically transparent thin-layer electrode) cell was composed of a 1 mm cuvette, a platinum gauze as the working electrode, a Ag/AgCl reference electrode and a platinum wire as the auxiliary electrode.

Materials

The supporting electrolyte was tetra-*n*-butylammonium perchlorate (TBAP) purchased from Aldrich. TBAP was first recrystallized from ethyl acetate and then dried *in vacuo*. Tetramethylammonium hydroxide TMA(OH) (Aldrich, 99%), cyclohexene (Jassen, 99%) and styrene were used as received. Acetonitrile (CH_3CN) was received as HPLC grade and was distilled over calcium hydride prior to use. Chloro-(5,10,15,20-tetraphenylporphyrinato) manganese(III) ($Mn^{III}TPP(Cl)$) was synthesized by the method used by Alder,[12] using chlorin-free H_2TPP (Aldrich, 99%) and $MnCl_2{\cdot}4H_2O$. Chloro-(2,3,7,8,12,13,17,18-octaethylporpyrinato) manganese(III) ($Mn^{III}OEP(Cl)$) and chloro-(5,10,15,20-tetrakis(pentafluorophenyl)porphyrinato) manganese(III) ($Mn^{III}TpFPP(Cl)$) were synthesized in the same way. $Mn^{III}TPP(OAc)$, $Mn^{III}OEP(OAc)$ and $Mn^{III}TpFPP(OAc)$ were synthesized in the same way except that $Mn(OAc)_2{\cdot}4H_2O$ was used. Synthesis of $Mn^{III}TPP(ClO_4)$ was achieved by gentle reflux of a equimolar amount of $Mn^{III}TPP(Cl)$ and $AgClO_4$ in benzene for one hour.[10,13] $Mn^{III}OEP(ClO_4)$ and $Mn^{III}TpFPP(ClO_4)$ were synthesized in the same way. $Mn^{III}TPP(OH)$ was synthesized using $Mn^{III}TPP(Cl)$ and excess TMA(OH) in acetonitrile. The mixture was stirred for 30 min and the solvent was evaporated. The resulting solid was dissolved in dichlomethane and washed with a large volume of water to remove the additional TMA(OH). $Mn^{III}TPP(OH)$ was obtained after dichloromethane was evaporated.

RESULTS AND DISCUSSION

Reduction of $Mn^{III}P(X)$

Fig. 1 shows the cyclic voltammograms of $Mn^{III}TPP(X)$ (X = OH^-, ClO_4^-, Cl^- and OAc^-) in CH_3CN. Two well-defined reduction waves were obtained. The first one ranging from -0.33 to -0.15 V corresponds to the one-electron reduction of the central metal ion.[10,14] The second one between -1.26 and -1.43 V can be assigned as the one electron reduction of the porphyrin ring and thus the formation of the anion radical.[10]

The observed potentials for all reactions in Fig. 1 are tabulated in Table 1. The redox potentials of $Mn^{III}TPP(ClO_4)$ and $Mn^{III}TPP(Cl)$ are in general agreement with those reported in the literature.[10] Reported potential for the first reduction in CH_3CN was -0.19 and -0.23 V vs. SCE, respectively. As seen in this table, the reduction of $Mn^{III}TPP(X)$ was almost the same for X = Cl^-, ClO_4^- and OH^-, which indicates a similar interaction between Mn(III) and the counterion in CH_3CN. The reduction potential of $Mn^{III}TPP(OAc)$ is more positive than that of $Mn^{III}TPP(ClO_4)$ by 0.12 V. Because of the coordination effect of CH_3CN, the binding strength of ClO_4^-, Cl^- and OH^- is not significant. The Mn(III)-counter ion binding strength is thus $OAc^- < ClO_4^- \sim Cl^- \sim OH^-$.

As seen in Table 1, however, the ligation effect on redox potential of $Mn^{III}OEP(X)$ and $Mn^{III}TpFPP(X)$ (X= ClO_4^-, Cl^- and OAc^-) are slightly different from $Mn^{III}TPP(X)$.

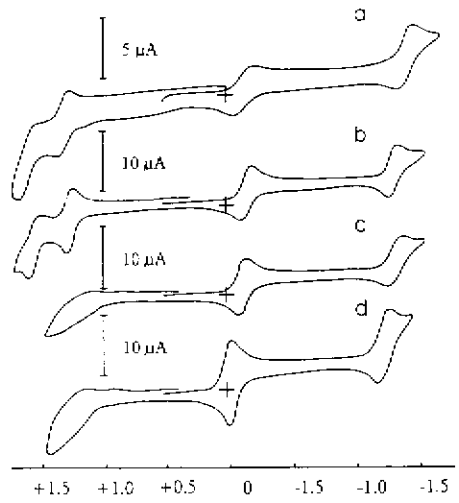

Fig. 1. Cyclic voltammograms of manganese porphyrins in CH_3CN with 0.1 M TBAP, scan rate = 100 mV/s. (a) $Mn^{III}TPP(OH)$ (b) $Mn^{III}TPP(ClO_4)$ (c) $Mn^{III}TPP(Cl)$ (d) $Mn^{III}TPP(OAc)$.

Table 1. Redox Potentials of Manganese Porphyrins in CH_3CN Containing 0.1 M TBAP

	$Ring_{ox2}$	$Ring_{ox1}$	$Mn^{IV/III}$	$Mn^{III/II}$	$Ring_{red1}$	$Ring_{red2}$
$Mn^{III}TPP(OAc)$	no[d]	no[d]	no[d]	-0.03	-1.26	no[d]
$Mn^{III}TPP(Cl)$	no[d]	no[d]	no[d]	-0.14	-1.36	no[d]
$Mn^{III}TPP(ClO_4)$	+1.57	+1.30	no[d]	-0.15	-1.33	no[d]
$Mn^{III}TPP(OH)$	+1.60	+1.34	no[d]	-0.13	-1.43	no[d]
$Mn^{III}TPP(OH)_2$	no[d]	no[d]	+0.43	-0.70[a]	-1.43	no[d]
$Mn^{III}OEP(OAc)$	no[d]	no[d]	no[d]	-0.35	no[d]	no[d]
$Mn^{III}OEP(Cl)$	no[d]	no[d]	no[d]	-0.36	no[d]	no[d]
$Mn^{III}OEP(ClO_4)$	+1.34	+1.16	no[d]	-0.29	no[d]	no[d]
$Mn^{III}OEP(OH)_2$	no[d]	no[d]	+0.22	no[d]	no[d]	no[d]
$Mn^{III}TpFPP(OAc)$	no[d]	no[d]	no[d]	+0.04	-1.06	-1.37
$Mn^{III}TpFPP(Cl)$	no[d]	no[d]	no[d]	-0.04	-1.14	-1.52
$Mn^{III}TpFPP(ClO_4)$	no[d]	no[d]	no[d]	+0.05	-1.19	-1.37
$Mn^{III}TpFPP(OH)_2$	no[d]	no[d]	+0.77[b]	-0.41[c]	-1.03	no[d]

[a] quasi-reversible $E_{p,a}$ = -0.63 V, $E_{p,c}$ = -0.77 V.
[b] quasi-reversible $E_{p,a}$ = +0.81 V, $E_{p,c}$ = +0.73 V.
[c] quasi-reversible $E_{p,a}$ = -0.34 V, $E_{p,c}$ = -0.48 V.
[d] no = not observed.

The $Mn^{III/II}OEP(X)$ redox potentials occurred at more negative potentials than those of $Mn^{III/II}TPP(X)$. $Mn^{III}OEP(ClO_4)$ is reduced at -0.29 V, which is more positive than that of $Mn^{III}OEP(OAc)$ and $Mn^{III}OEP(Cl)$. The Mn(III)-counterion binding strength is ClO_4^- < OAc^- ~ Cl^-. The $Mn^{III/II}TpFPP(X)$ redox potentials occurred at more positive potentials than those of $Mn^{III/II}TPP(X)$. The electron-withdrawing effect of the five fluorine atoms at the phenyl group makes the central metal ion reduction easier. $Mn^{III}TpFPP(OAc)$ and $Mn^{III}TpFPP(ClO_4)$ were reduced at +0.04 and +0.05 V, respectively. This suggests a similar ligation ability of OAc^- and ClO_4^-. $Mn^{III}TpFPP(Cl)$ is reduced at -0.04 V, which indicates a stronger ligation ability than that of ClO_4^- and OAc^-. Thus, the binding strength is OAc^- ~ ClO_4^- < Cl^-.

The second reduction waves were observed for $Mn^{III}TPP(X)$ and $Mn^{III}TpFPP(X)$ systems. In the $Mn^{III}OEP(X)$ system, no ring reduction was observed. This might result from the more conjugated porphyrin ring of the TPP system over that of the OEP system. Owing to the electron-withdrawing effect, there can be third reduction waves observed for the MnTpFPP system. The second and the third reductions correspond to the porphyrin ring reductions to form anion and dianion radicals, respectively.[15,16]

Oxidation of $Mn^{III}P(X)$

The oxidation of $Mn^{III}TPP(X)$ is shown in Fig. 1. The first oxidation waves of $Mn^{III}TPP(OH)$ and $Mn^{III}TPP(ClO_4)$ are well-defined and reversible. The redox potentials are at +1.34 and +1.30 V, respectively. The second oxidation waves are quasi-reversible. The oxidation sites involved the porphyrin ring system to yield Mn(III) cation radicals and dications, respectively.[15,16] The oxidation waves of $Mn^{III}TPP(Cl)$ and $Mn^{III}TPP(OAc)$ are, however, irreversible.

Time-resolved spectra of $Mn^{III}TPP(OAc)$ at +1.05 V is shown in Fig. 2. The absorbance of Soret band at 374 and 474 nm decreased, and the new peak at 388 nm grew up. The isosbestic points were distinct, indicating that only two species were present in appreciable quantities during this transformation. The final spectrum is identical with that of

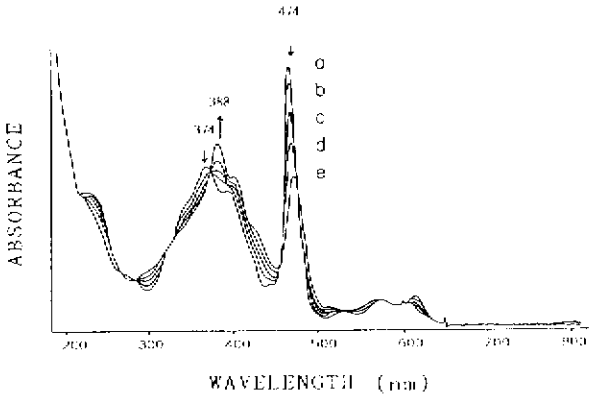

Fig. 2. Time-resolved spectra of 8×10^{-5} M $Mn^{III}TPP(OAc)$ at $E_{applied}$ = +0.95 V in CH_3CN with 0.1 M TBAP. Time = (a) 0 (b) 1.5 (c) 3.0 (d) 7.0 (e) 14 min.

$Mn^{III}TPP(ClO_4)$. The spectrum would be not changed if the solution stands for 24 hours without applying oxidation potential. In the cyclic voltammogram of $Mn^{III}TPP(OAc)$ (Fig. 1d), there isn't any oxidation reaction occurring at E < +1.05 V. Bulk electrolysis of $Mn^{III}TPP(OAc)$ at +1.05 V results in the axial ligand replacement of OAc^- by ClO_4^- coming from the supporting electrolyte. This is the first case of electrochemically induced axial ligand exchange of $Mn^{III}TPP(X)$. In the case of $Mn^{III}TPP(Cl)$ and $Mn^{III}TPP(OH)$, ClO_4^- replacement of the axial ligand was also observed at +1.05 and +0.95 V, respectively. And $Mn^{III}TPP(ClO_4)$ is finally produced.

Fig. 3 illustrates the spectral change of $MnTPP(ClO_4)$ at various oxidation potentials. ClO_4^- is chosen as the axial ligand because the other ligands such as OAc^-, Cl^- and OH^- would be replaced by ClO_4^- during electrolysis. The spectral changes should be simpler for ClO_4^- as an axial ligand. The absorbance at 388 and 486 nm decreased. The final spectrum exhibited a broad band between 600 to 700 nm, which is typical for a porphyrin cation radical. The calculated formal potential is +1.25 V,[17] slightly different from that in the cyclic voltammogram.

Hydroxide Anion Coordination with $Mn^{III}P(X)$

Fig. 4 illustrates the spectral change of $Mn^{III}TPP(ClO_4)$ during the titration with TMA(OH) in CH_3CN. The peak at 486 nm is blue-shifted and a new peak arises at 468 nm. The absorbance at 388 nm decreases and the peak becomes broader. A shoulder arises at 494 nm. The absorbance at 494 nm reaches a maximum until $[TMA(OH)]/[Mn^{III}TPP(ClO_4)]$ = 1.5 (Fig. 4A). Further addition of TMA(OH) causes the decrease of absorbance at 468 and 494 nm and the appearance of peaks at 410 and 430 nm. The absorbance at 410 and 430 nm reaches maxima at $[TMA(OH)]/[Mn^{III}TPP(ClO_4)]$ = 8. The absorption spectrum remains unchanged upon the addition of more TMA(OH) (Fig. 4B). The phenomena indicate that hydroxide anion ligated to Mn^{III} center during the titration process. The predominant species is $Mn^{III}TPP(OH)$ at $[TMA(OH)]/[Mn^{III}TPP(ClO_4)]$ = 1.5 and is $Mn^{III}TPP(OH)_2$ at $[TMA(OH)]/[Mn^{III}TPP(ClO_4)]$ = 8.0. The formation constants are thus estimated from the spectrophotometric titration.[18]

$$Mn^{III}TPP(ClO_4) + OH^- = Mn^{III}TPP(OH) + ClO_4^-$$
$$\log K_1 = 6.1 (\pm 0.3)$$
$$Mn^{III}TPP(OH) + OH^- = Mn^{III}TPP(OH)_2^-$$
$$\log K_2 = 4.0 (\pm 0.3)$$

The spectral change of direct titration of $Mn^{III}TPP(OH)$ with TMA(OH) also indicates the axial ligation of the second hydroxide anion. The absorbance at 382, 468 and 494 nm decreases while that at 410 and 430 nm increases. The final spectrum is identical to that of $Mn^{III}TPP(OH)_2$. The calculated formation constant, log K_2 = 3.7, is very close to

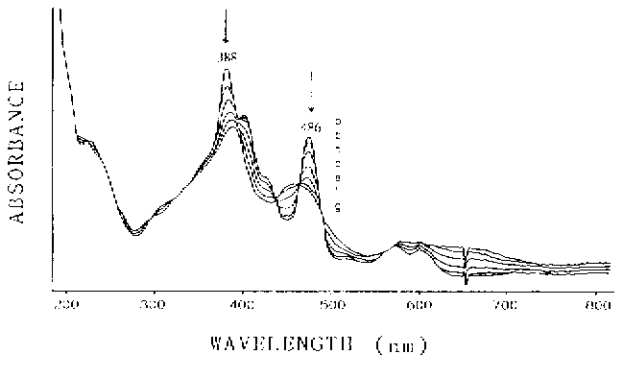

Fig. 3. Thin-layer spectra of 6×10^{-5} M $Mn^{III}TPP(ClO_4)$ in CH_3CN with 0.1 M TBAP. $E_{applied}$ = (a) 1.15 (b) 1.18 (c) 1.21 (d) 1.24 (e) 1.27 (f) 1.30 (g) 1.33 V.

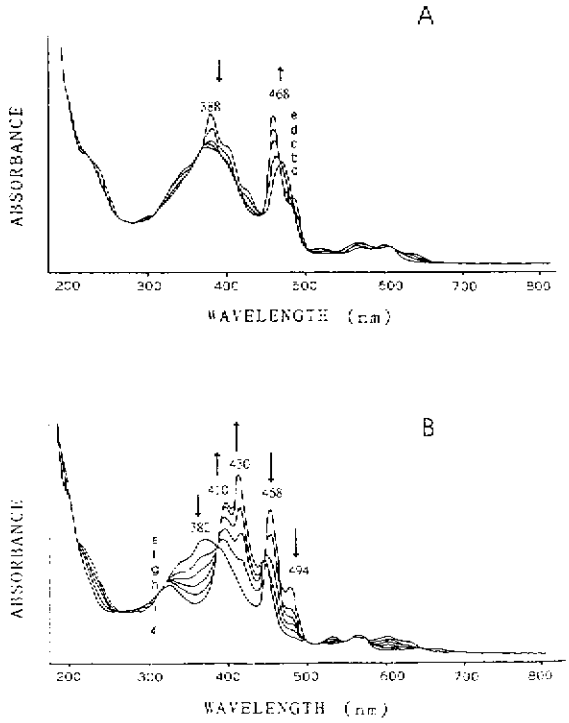

Fig. 4. Absorption spectra of 1×10^{-4} M $Mn^{III}TPP(ClO_4)$ titrated with TMA(OH) in CH_3CN. $[TMA(OH)]/[Mn^{III}TPP(ClO_4)]$ = (a) 0 (b) 0.3 (c) 0.6 (d) 1.0 (e) 1.5 (f) 2.5 (g) 3.5 (h) 4.6 (i) 5.8 (j) 8.0.

that obtained from Fig. 4.

The spectral change in the titration of $Mn^{III}OEP(Cl)$ with TMA(OH) proceeds in a similar pattern. The absorbance at 488 nm arose at first and decreased gradually, which suggests the formation of $Mn^{III}OEP(OH)$ and $Mn^{III}OEP(OH)_2$, respectively. The formation of monohydroxide and dihydroxide coordinated manganese porphyrin depends on the [TMA(OH)]/[$Mn^{III}OEP(Cl)$] ratio. The predominant species is $Mn^{III}OEP(OH)$ at [TMA(OH)]/[$Mn^{III}OEP(Cl)$] = 2.0, and is $Mn^{III}OEP(OH)_2$ at [TMA(OH)]/[$Mn^{III}OEP(Cl)$] = 35.0. The formation constants are log K_1 = 5.2 (± 0.3) and log K_2 = 3.0 (± 0.3), respectively.

In the titration of $Mn^{III}TpFPP(Cl)$ with TMA(OH), the pattern of spectral change differs from those of the $MnTPP(ClO_4)$ and MnOEP(Cl). Rather, the Soret bands at 360 and 470 nm decrease and a broad band at 430 nm increases monotonously. No isosbestic point is observed in this wavelength region. This may result from the same order of the formation constants for the monohydroxide and dihydroxide ligation on $Mn^{III}TpFPP(Cl)$. The spectrum is no longer changed at [TMA(OH)]/[$Mn^{III}TpFPP(Cl)$] > 3.2. Under this condition, presumably $Mn^{III}TpFPP(OH)_2$ is formed.

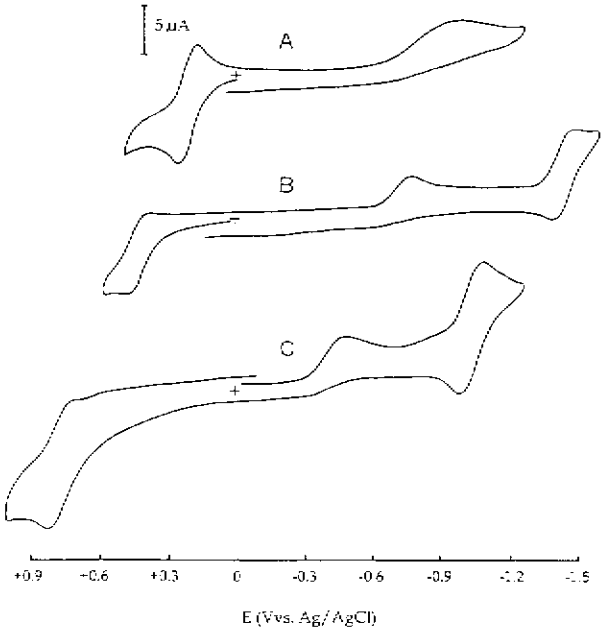

Fig. 5. Cyclic voltammograms of (A) 4.4 × 10^{-4} M $Mn^{III}OEP(OH)_2$, [TMA(OH)]/[$Mn^{III}OEP(Cl)$] = 35 (B) 6 × 10^{-4} M $Mn^{III}TPP(OH)_2$, [TMA(OH)]/[$Mn^{III}TPP(ClO_4)$] = 8 (C) 7.0 × 10^{-4} M $Mn^{III}TpFPP(OH)_2$ [TMA(OH)/[MnTpFPP(Cl)] = 3.2 in CH_3CN with 0.1 M TBAP, scan rate = 100 mV/s.

Electrochemical Properties of $Mn^{III}P(OH)_2$

A cyclic voltammogram of $Mn^{III}OEP(OH)_2$ is shown in Fig. 5A. A redox couple occurs at $E_{1/2}$ = +0.22 V. The spectral change of $Mn^{III}OEP(OH)_2$ at various oxidation potentials is shown in Fig. 6. The absorbance at 362 and 420 nm decreases while that at 400 nm increases, and the spectrum is similar to that of oxomanganese(IV) porphyrin previously reported.[19] The spectrum remains unchanged and the species is stable at +0.35 V. At +0.00 V, the spectrum returns to that of $Mn^{III}OEP(OH)_2$ without significant loss of absorbance. The redox couple at +0.22 V is thus assigned as the metal center oxidation.

$$Mn^{III}OEP(OH)_2 = O{=}Mn^{IV}OEP(OH) + e^- + H^+$$
$$E_{1/2} = +0.22\ V$$

Fig. 5B shows the cyclic voltammogram of $Mn^{III}TPP(OH)_2$ in CH_3CN. A quasi-reversible redox couple is observed at +0.43 V. The oxidation of hydroxide at the glassy carbon electrode starts at +0.5 V, and the redox couple apparently overlaps with the irreversible oxidation wave of hydroxide. OTTLE measurement at +0.53 V shows that the absorbance at 410, 430 and 468 nm decreases gradually and the peak shifts to 400 nm, which is similar to the reported spectrum of $O{=}Mn^{IV}TPP(OH)$.[19] The oxidation reaction is thus inferred as the metal oxidation.

$$Mn^{III}TPP(OH)_2 = O{=}Mn^{IV}TPP(OH) + e^- + H^+$$
$$E_{1/2} = +0.43\ V$$

The absorbance at 400 nm of the oxidized form, however, decreased gradually, indicating the decompositon of oxomanganese(IV) porphyrin. It has been reported that

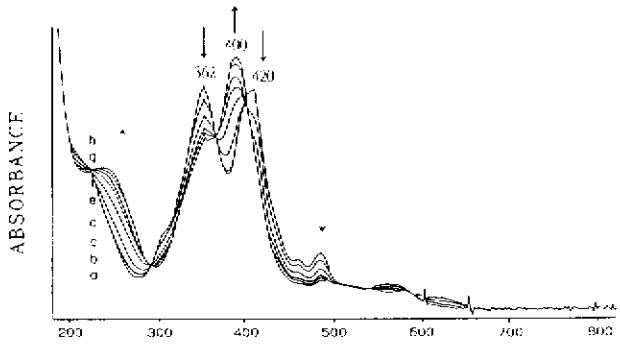

Fig. 6. Thin-layer spectra of 1 × 10^{-4} M $Mn^{III}OEP(OH)_2$ in CH_3CN with 0.1 M TBAP. [TMA(OH)]/[$Mn^{III}OEP(Cl)$] = 35. $E_{applied}$ = (a) 0.14 (b) 0.17 (c) 0.20 (d) 0.23 (e) 0.26 (f) 0.29 (g) 0.32 (h) 0.35 V.

$O=Mn^{IV}TPP(OH)$ is unstable in room temperature,[8] so that the absorption spectrum of oxomanganese(IV) porphyrin changes gradually without an isosbestic point during the electrolysis. Probably the OH^- oxidation products react with the porphyrin and cause decomposition.

Cyclic voltammetry of $Mn^{III}TpFPP(OH)_2$ (Fig. 5C) shows a similar pattern as that of $MnTPP(OH)_2$. The oxidation waves are obscured by that of hydroxide oxidation. Owing to the electron-withdrawing effect of fluorine atoms, the oxidation potential occurred at about $E_{1/2}$ = +0.77 V, which is more positive than that of $Mn^{III}TPP(OH)_2$. Electrolysis of $Mn^{III}TpFPP(OH)_2$ at +0.65 V for 30 min does not cause spectral change. But the spectrum finally becomes that of $Mn^{III}TpFPP(Cl)$. Hydroxide in TMA(OH) solution is oxidized at +0.65 V. During the electrolysis processes, TMA(OH) is consumed. After TMA(OH) is exhausted in the solution, $Mn^{III}TpFPP(Cl)$ reappeared.

Electrooxidation of $Mn^{III}P(OH)_2$ in the Presence of Alkenes

The absorption spectral change of $Mn^{III}OEP(OH)_2$ in the presence of styrene at +0.32 V is shown in Fig. 7. An absorption peak at 406 nm appeared with distinct isosbestic points during electrolysis for about 12 min, indicating the formation of the oxomanganse(IV) porphyrin. It is a little red-shifted from the spectral change in the absence of styrene (Fig. 6). In the continuation of electrolysis, the absorption spectrum changes in a reverse direction (Fig. 7B). $Mn^{III}OEP(Cl)$ reappeared as evidenced by the absorption peaks at 356 and 468 nm. The results suggest an oxygen atom transfer from oxomanganese(IV) porphyrin to styrene. After the oxygen source is consumed, only $Mn^{III}OEP(Cl)$ is present and is not oxidized at +0.32 V. The absorbance of $Mn^{III}OEP(Cl)$ before and after electrolysis is almost the same, indicating no significant decomposition of $Mn^{III}OEP(Cl)$ in the presence of styrene during electrolysis. Electrolysis of $Mn^{III}OEP(OH)_2$ in the presence of cyclohexene exhibits the same pattern for spectral change. It is evident that oxomanganese(IV) porphyrin is capable of transferring an oxygen atom to alkenes.

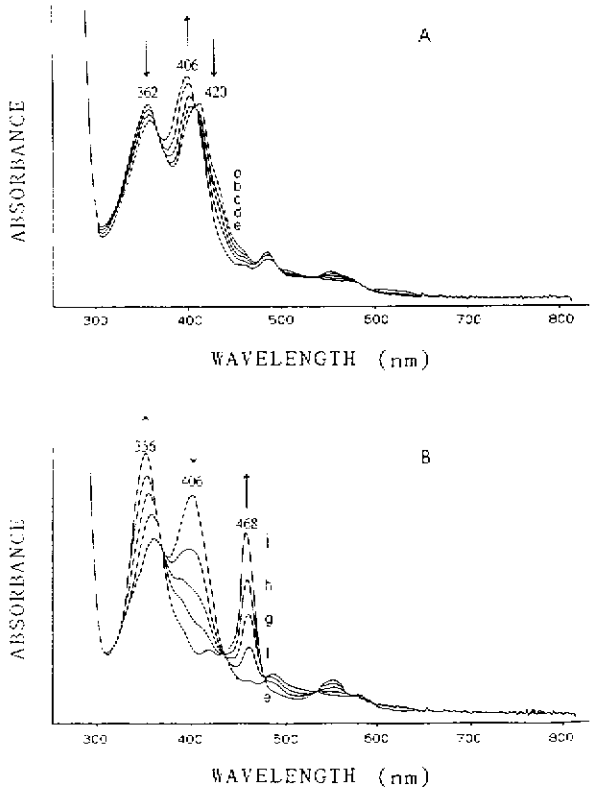

Fig. 7. Thin-layer spectra of 1×10^{-4} M $Mn^{III}OEP(OH)_2$ containing 50 mM styrene in CH_3CN with 0.1 M TBAP. [TMA(OH)]/[$Mn^{III}OEP(Cl)$] = 35. $E_{applied}$ = +0.32 V. Time = (a) 0 (b) 0.5 (c) 1.5 (d) 6 (e) 12 (f) 32 (g) 57 (h) 87 (i) 187 min.

$O=Mn^{IV}TPP(OH)$ also acts as an active species in the catalytic oxidation of alkene. In the presence of styrene or cyclohexene, the absorption peak at 400 nm appeared at electrolysis for about 15 min with distinct isosbestic points. It is totally different from the decomposition situation in the absence of alkenes. That is to say, $O=Mn^{IV}TPP(OH)$ is stabilized in the presence of alkenes. After electrolysis for 1 hour, $Mn^{III}TPP(ClO_4)$ spectrum reappeared. The ligation with OH^- and oxidation reactions with alkenes for manganese porphyrins are thus summarized in Scheme I.

Scheme I

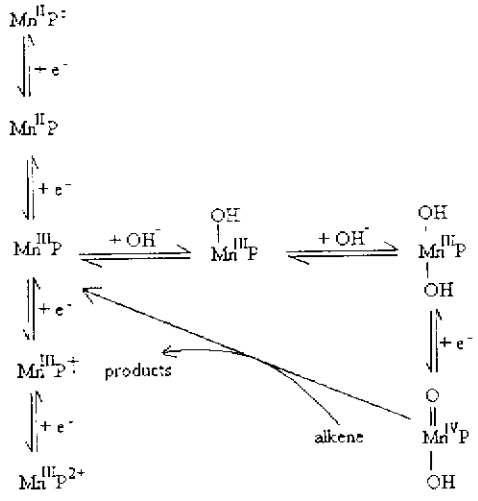

P = TPP or OEP

ACKNOWLEDGMENT

This work was supported by the National Science Council of the Republic of China.

Received November 3, 1998.

Key Words

Manganese porphyrin; Redox reaction; Axial ligand; Alkene.

REFERENCES

1. Boucher, L. J. *Coord. Chem. Rev.* **1972**, *7*, 289.
2. Schardt, B. C.; Hollander, F. J.; Hill, C. L. *Inorg. Chem.* **1983**, *22*, 3776.
3. Camenzind, M. J.; Hill, C. L.; Hollander, F. J. *Inorg. Chem.* **1983**, *22*, 3776.
4. Hill, C. L.; Hollander, F. J. *J. Am. Chem. Soc.* **1982**, *104*, 7318.
5. Buchler, J. W.; Dreher, C.; Lay, K.-L.; Lee, Y. J. A.; Scheidt, W. R. *Inorg. Chem.* **1983**, *22*, 888.
6. Dunford, H. P. *Adv. Inorg. Biochem.* **1982**, *4*, 41.
7. Meunier, B. *Chem. Rev.* **1992**, *92*, 1411.
8. Groves, J. T.; Stern, M. K. *J. Am. Chem. Soc.* **1988**, *110*, 8628.
9. Liu, M.-H.; Yeh, C.-Y.; Su, Y. O. *Chem. Commun.* **1996**, 1473.
10. Kelly, S. L.; Kadish, K. M. *Inorg. Chem.* **1982**, *21*, 3631.
11. Mu, X. H.; Schultz, F. A. *Inorg. Chem.* **1992**, *31*, 3351.
12. Adler, A. D.; Longo, F. R.; Kampas, F.; Kim, J. *Inorg. Nucl. Chem.* **1970**, *32*, 2443.
13. Tsang, P. K. S.; Cofre, P.; Sawyer, D. T. *Inorg. Chem.* **1987**, *26*, 3604.
14. Boucher, L. J.; Garber, H. K. *Inorg. Chem.* **1970**, *9*, 2644.
15. Felton, R. H. in *The Porphyrins*, vol. 3, Dolphin, D. Ed.; Academic Press, New York, **1978**.
16. Fuhrhop, J. H. in *Porphyrins and Metalloporphyrins*, Smith, K. Ed.; Elsevier, New York, **1978**.
17. Rohrbach, D. F.; Deutsch, E.; Heineman, W. R.; Pasternack, R. F. *Inorg. Chem.* **1977**, *16*, 2650.
18. Kim, D.; Su, Y. O.; Spiro, T. G. *Inorg. Chem.* **1986**, *25*, 3988.
19. Suslick, K. S.; Acholla, F. V.; Cook, B. R. *J. Am. Chem. Soc.* **1987**, *109*, 2818.